Journal of Quantitative Spectroscopy & Radiative Transfer 215 (2018) 1–8

Contents lists available at ScienceDirect

Journal of Quantitative Spectroscopy & Radiative Transfer

journal homepage: www.elsevier.com/locate/jqsrt

Applying machine learning to estimate the optical properties of black carbon fractal aggregates

Jie Luo, Yongming Zhang, Feng Wang, Jinjun Wang, Qixing Zhang*

State Key Laboratory of Fire Science, University of Science and Technology of China, Hefei, Anhui 230026, China

ARTICLE INFO

Article history:
Received 3 December 2017
Revised 2 May 2018
Accepted 2 May 2018
Available online 3 May 2018

Keywords:
Black carbon aggregates
Optical properties
Support vector machine
Morphology
T-matrix

ABSTRACT

Calculation of the optical properties of black carbon fractal aggregates is important in a variety of applications, whereas the complex morphology of black carbon aggregates makes it particularly computationally expensive for broadband applications. Previous studies have tried to parameterize the optical properties with empirical fitting. In this work, a machine learning method, support vector machine, was applied to estimate the optical properties. The integral optical properties obtained by numerically exact multiple-sphere T-matrix method and trained support vector machine model respectively, were presented and discussed in this study. The comparative results show excellent agreement between the two methods. Even though machine learning may provide inaccurate results when morphological parameters are beyond the range of training dataset, after adding small number of data on the basis of pre-trained support vector machine model to cover the full range, relative errors of extinction efficiency (Q_{ext}), absorption efficiency (Q_{abs}), scattering efficiency (Q_{sca}) and asymmetric factor (ASY) are within 2.3%, 1.4%, 5% and 4.8% respectively. The errors are acceptable because the MSTM results may fluctuate from mean values over a small range. Therefore, machine learning can reconstruct the full range of optical properties by small number of training data. This work provides a new method to estimate optical properties of black carbon aggregates and is helpful for simplifying the calculation of optical properties of black carbon fractal aggregates. It may be helpful for atmospheric models calculations, aerosol optical inversions and other fields involved in calculation of BC aggregates with broadband morphological parameters. Moreover, it may provide a new insight for parameterizations of optical properties of BC with more complex morphologies.

1. Introduction

Black carbon(BC), a product of incomplete combustion, makes the second largest contribution after CO_2 to climate forcing [1,2]. Calculation of the optical properties of BC aggregates is essential in a variety of applications such as optical diagnostics for combustion [3], climate studies [4–6], remote sensing [7,8] and fire detection [9,10]. However, it is a tremendous work to calculate the optical properties of BC aggregates due to the complex morphology.

Studies have shown that the BC aggregates are composed of numbers of BC monomers [11]. The construction of the structure satisfies the well-known fractal laws [12]:

$$n_s = k_0\left(\frac{R_g}{a}\right)^{D_f} \tag{1}$$

$$R_g^2 = \frac{1}{n_s}\sum_{i=1}^{n_s} l_i^2 \tag{2}$$

where n_s is the number of the monomers in the cluster, a is the mean radius of the monomer, k_0 is the fractal prefactor, D_f is the fractal dimension, R_g is the radius of gyration, and l_i is the distance from the ith monomer to the centre of the cluster.

However, the fractal parameters varies with the combustion conditions, fuel species and atmospheric aging status, which leads very complex morphology of BC aggregates. Numerical solution methods for Maxwell's equations, such as generalized multi-particle Mie (GMM) method [13,14], numerically exact multiple-sphere T-matrix (MSTM) method [15,16] and discrete-dipole approximation (DDA) method [17,18], are commonly applied to calculate the scattering properties of BC aggregates, which can result in huge computation cost when the fractal parameters are at a wide range. Therefore, it limits the study on the optical properties of BC aggregates.

For simplifying the calculation, Mie theory [19] is widely applied in climate model. However, it may introduce large errors due to over-simplification of the morphology [20–26]. Moreover, Smith et al. [27] found that it is difficult to find a sphere to fit the optical properties of BC aggregates. Consequently, parameterizations

* Corresponding author.
E-mail address: qixing@ustc.edu.cn (Q. Zhang).

https://doi.org/10.1016/j.jqsrt.2018.05.002
0022-4073/

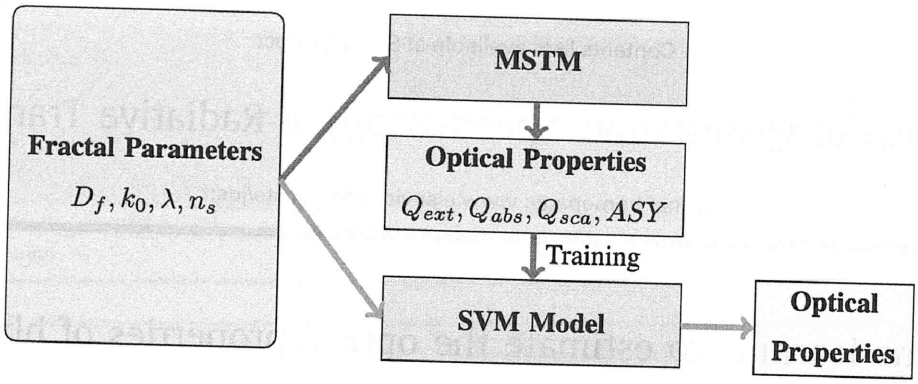

Fig. 1. The scheme of this study.

for optical properties of BC aggregates have gained increasing interests [27–31]. Based on the theoretical methods (e.g. T-matrix, DDA, etc.), we gain a physical insight on how fractal parameters affect BC optical properties, but for application, it is more convenient to use a direct parameterization to relate optical properties with particle morphology.

Kahnert et al. [28,29] parameterized BC aerosol optical properties (*AOP*) with volume equivalent radius (R_v) by using the third order polynomial. However, as pointed by Smith et al. [27], unsuccessful fits were found in scattering cross section (C_{sca}), $ASY \times C_{sca}$ and backscatter cross section. In the work of Smith et al. [27], nonlinear fits with n_s were used, and they found good parameterizations for a lognormal distribution of particles for full range of λ, D_f. However, they didn't consider the influences of k_0 and only single refractive index and monomer radius were considered in their work. Therefore, whether the parameterizations are suitable for other refractive indices and monomer radius is unexpected. Consequently, there is a need to find a method with extensive applicability. A machine learning method, support vector machine (SVM) [32], was used because the parameterization depends only on a subset of the training data but not limited by the range of fractal parameters. The aim is to transform the numerical methods to a parametrization network, and the scheme is shown in Fig. 1. This work applies the machine learning to link BC optical properties with its fractal morphology for the first time and provides a new insight to calculate the properties of BC aggregates.

The method for calculating the optical properties of the BC aggregates is introduced in Section 2. The theory of SVM and the application in parameterization of optical properties of BC aggregates are introduced in Section 3. The comparison results of SVM and MTSM are conducted in Section 4, discussions and future work are discussed in Section 5.

2. Calculation of optical properties of BC aggregates

2.1. Generation of BC aggregates

Diffusion-limited algorithms (DLA), including particle-cluster aggregation (PCA) [33] and cluster-cluster aggregation (CCA) methods [34], have been commonly applied to generate BC aggregates. In this work, a tunable DLA code developed by Wozniak et al. [35,36] was used. Compared with ordinary DLA code, it preserves fractal parameters at each step of the aggregation, which voids the generation of multi-fractal aggregates [37]. According to the SEM and TEM images, BC aggregates are composed of numbers of BC monomers and the monomer radius are commonly within $0.01 - 0.025um$ [11]. The monomer radius of BC aggregate was assumed to be $0.02um$ in this work even though the optical properties of BC particles is influenced by polydispersity of BC monomers [38–41]. The D_f can be used to evaluate the compactness of BC aggregates. The shape of BC aggregates becomes more compact when increasing the value of D_f. The typical reconstruction shapes of BC aggregates for different D_f are shown in Fig. 2. For the bare BC aggregates, it is commonly with chain-like shape, where small values of D_f are found, so the values of $D_f = 1.8 - 2.2$ were considered in this study. The $1.2 \le k_0 \le 1.6$ was assumed according to previous studies [42,43].

2.2. Calculation method

MSTM method has been developed to calculate the arbitrary configurations of spheres without overlapping [15,44,45]. Different from other numerical methods, the MSTM method calculates the optical properties of randomly oriented particles analytically without numerical averaging over particle orientations, so the efficiency is higher than most other numerical methods such as discrete dipole approximation (DDA) method [46]. Recently, the integral optical characteristics of BC aggregate have gained more and more attentions [41,47–49] for their essential contribution to calculations of the global radiation forcing. Different from previous study, the dimensionless optical efficiency factor are calculated in this work by dividing the optical cross section by the geometrical cross section [12]:

$$Q_{ext} = \frac{C_{ext}}{\pi R_v^2} \tag{3}$$

$$Q_{abs} = \frac{C_{abs}}{\pi R_v^2} \tag{4}$$

$$Q_{sca} = \frac{C_{sca}}{\pi R_v^2} \tag{5}$$

where C_{ext}, C_{abs} and C_{sca} represent extinction, absorption and scattering cross section respectively; R_v is the equivalent volume radius of an aggregate.

In this work, integral optical properties including Q_{ext}, Q_{abs}, Q_{sca} and *ASY* were calculated using the MSTM method. Due to that there are many configurations that satisfy identical fractal law, the optical properties may be varied over a small range. The deviation caused from random clusters can be reduced by averaging over multiple realizations. However, for simplifying the calculation, the optical properties of random aggregates were only calculated once.

3. Support vector machine(SVM)

SVM is a supervised learning model with associated learning algorithms that analyze data used for classification and regression analysis [32,50]. It was proposed by Vapnik [51] and it has been applied in multiple areas. Compared to other machine learning methods, SVM has an edge on solving non-linear problems due

(a) $D_f = 1.8$ (b) $D_f = 2.0$ (c) $D_f = 2.2$

Fig. 2. Typical fractal aggregates with $n_s = 200, k_0 = 1.2$.

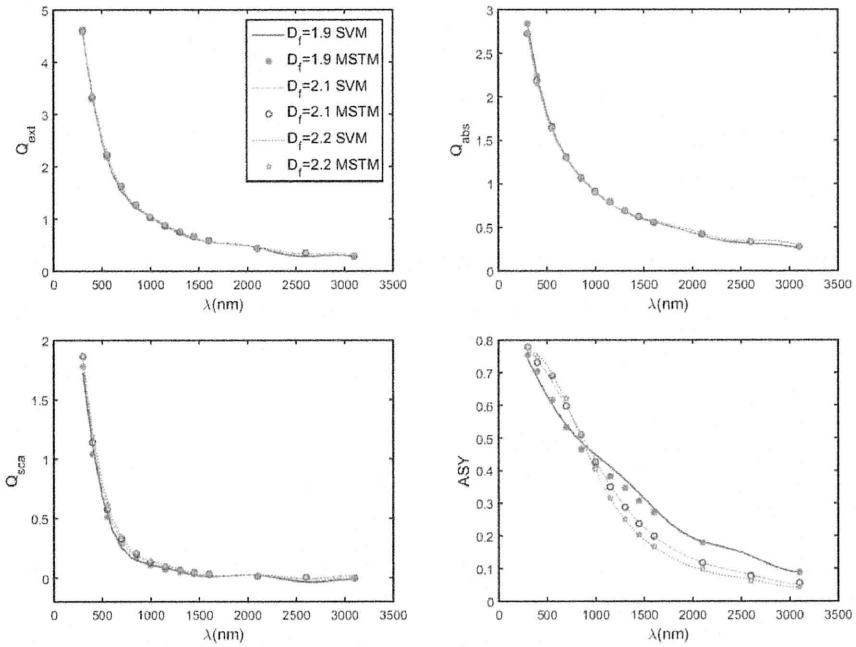

Fig. 3. Comparative results of MSTM and SVM varies with λ for different fractal dimensions, $n_s = 200, k_0 = 1.2, a = 20nm, m = 1.95 + 0.79i$.

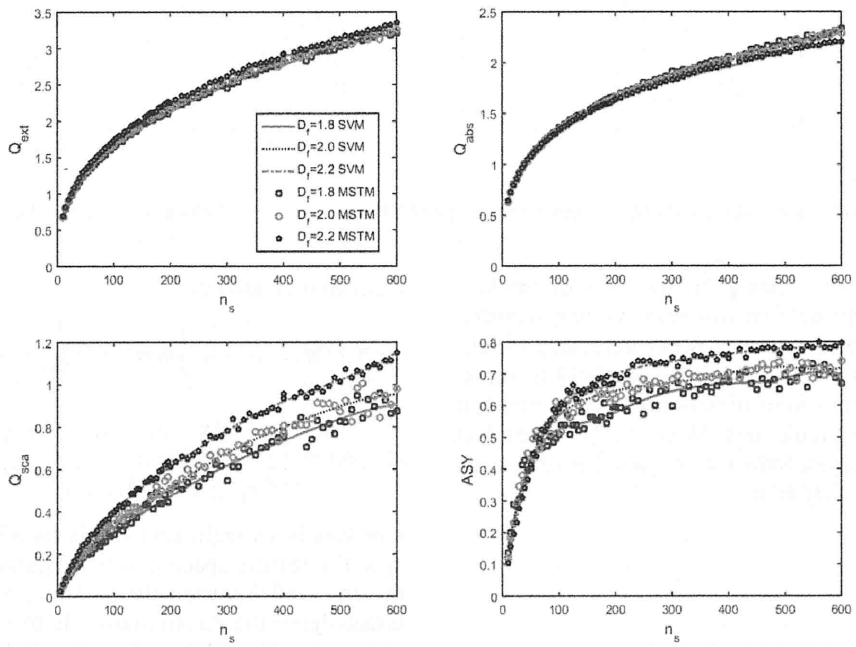

Fig. 4. Comparative results of MSTM and SVM varies with n_s for different fractal dimensions, $\lambda = 550nm, k_0 = 1.2$.

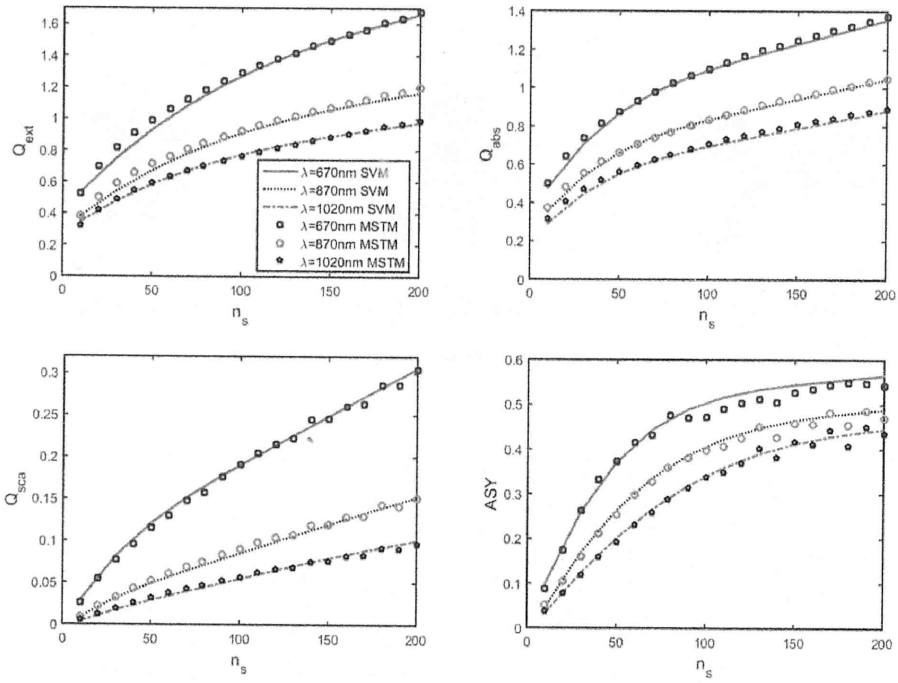

Fig. 5. Comparative results of MSTM and SVM, $k_0 = 1.37, D_f = 1.8, a = 20nm, m = 1.95 + 0.79i$.

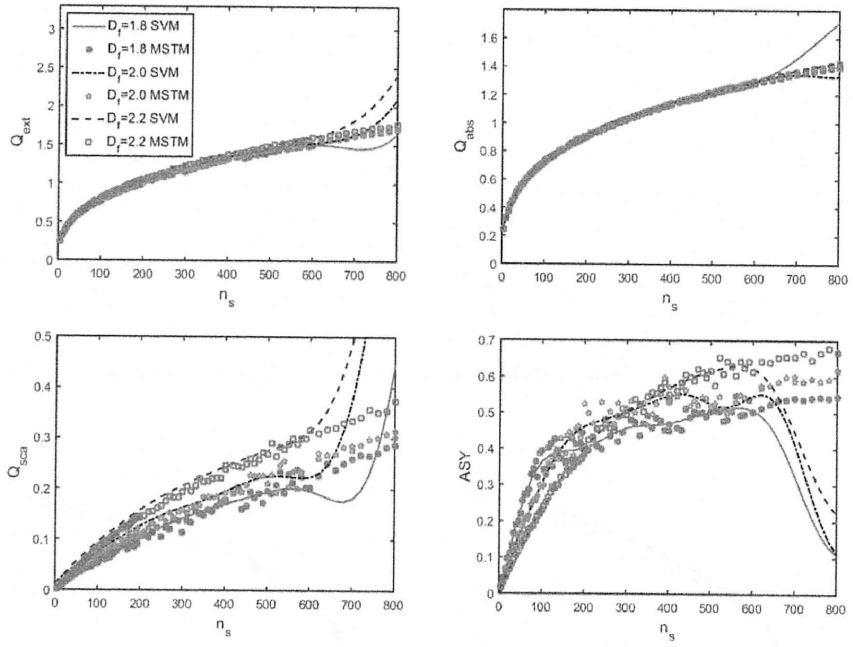

Fig. 6. Overfitting when the fractal parameters are beyond the scope of training dataset, $\lambda = 1000nm, k_0 = 1.2, a = 20nm, m = 1.95 + 0.79i$.

to the application of kernel functions [52]. The idea of the kernel function is to transform the data vectors from a low-dimension space to a high-dimension space where it is not necessary to represent the mapping function explicitly. This allows SVM to transform a non-linear problem into high dimensional linear problem so that gives more accurate predictions. SVM can be applied in both classification and regression. SVM was applied for regression by Drucker et al. [53] for the first time.

3.1. SVM for regression

The epsilon support vector regression (ε-SVR) was used in this study. Given a training dataset $\{(\boldsymbol{x}_1, y_1), \ldots, (\boldsymbol{x}_n, y_n)\}$, ε-SVR aims to fit a function with $\boldsymbol{x}$ by finding a prediction model. It can be expressed as follows:

$$\min_{w,\xi,\xi^*} \tau(\boldsymbol{w}, \xi, \xi^*) = \frac{1}{2}\boldsymbol{w}\boldsymbol{w}^T + C\sum_{i=1}^{n}\xi_i + C\sum_{i=1}^{n}\xi_i^* \tag{6}$$

$$subject = \begin{cases} w^T\Phi(\boldsymbol{x}_i) + b - y_i \le \epsilon + \xi_i, \\ y_i - w^T\Phi(\boldsymbol{x}_i) - b \le \epsilon + \xi_i^*, \\ \xi_i\xi_i^* \ge 0, i = 1, \ldots, n \end{cases} \tag{7}$$

where $\boldsymbol{w}$ is a weight vector, b is the bias and $\Phi(\boldsymbol{x}_i)$ maps the input $\boldsymbol{x}_i$ to the feature space. C is the regularization parameter to control the trade-off between the soft margins which allows a few data dissatisfying the constraints. ϵ is the amount up to which differences are tolerated. ξ and ξ^* are slack variables which are used to relax the constraints slightly to allow for bad estimations. The solution for the estimated value $\hat{y}_*$ at each new point $\boldsymbol{x}_*$, is given by:

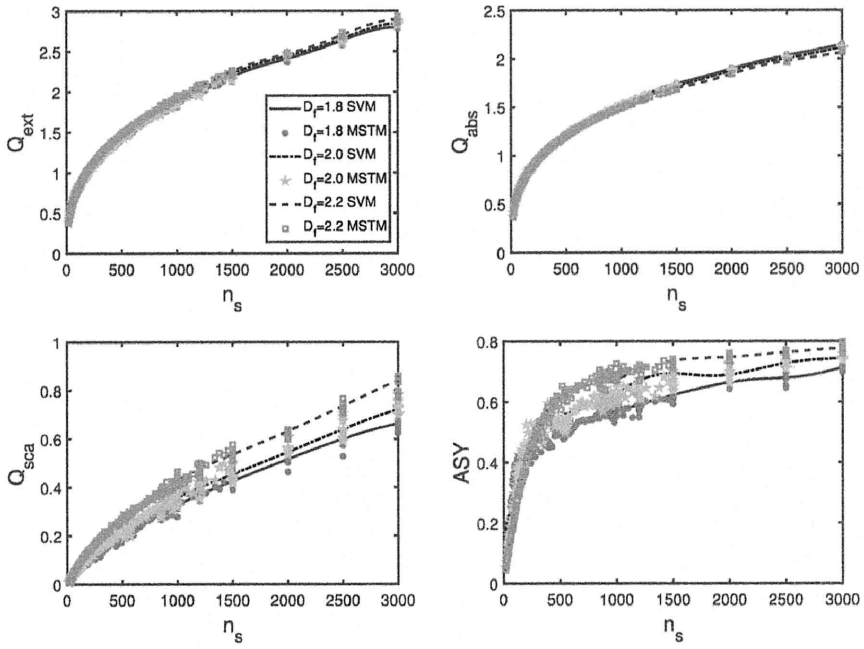

Fig. 7. Comparative results of SVM and MSTM when adding a few results to cover the whole fractal parameters range, $\lambda = 1000nm$, $k_0 = 1.2$, $a = 20nm$, $m = 1.95 + 0.79i$.

$$\hat{y}_* = \sum_{i=1}^{n}(-\alpha_i + \alpha_i^*)k(\boldsymbol{x}_i, \boldsymbol{x}_*) + b \tag{8}$$

where

$$k(\boldsymbol{x}_i, \boldsymbol{x}_j) = \Phi(\boldsymbol{x}_i)^T \Phi(\boldsymbol{x}_j)^T \tag{9}$$

Due to the nonlinear correlation between optical properties and fractal parameters, the radial basis function(RBF) [54] was used in this study. One of the most widely used SVM code LIBSVM [55] was applied to parametrize the optical properties of BC aggregates. The SVM model parameters are of great importance for the predicted results. To obtain a satisfactory parametrization, grid search for kernel parameters with cross validation [56] was applied in this study.

This work is aimed to find a direct relation between optical properties and the fractal parameters, and single refractive index m=1.95 + 0.79i was assumed. The training dataset was given in the form:

$$\boldsymbol{X} = [\boldsymbol{D_f} \quad \boldsymbol{k_0} \quad \boldsymbol{\lambda} \quad \boldsymbol{n_s}] \tag{10}$$

$$\boldsymbol{Y} = [\boldsymbol{Q_{ext}} \quad \boldsymbol{Q_{abs}} \quad \boldsymbol{Q_{sca}} \quad \boldsymbol{g}] \tag{11}$$

where $\boldsymbol{X}$, $\boldsymbol{Y}$ are $n \times 4$ matrix, and n is the number of calculation results. The $\boldsymbol{g}$ represents the results of asymmetry factor. We calculated the optical properties using MSTM method, and the results are trained in the form $[\boldsymbol{X}, \boldsymbol{Q_{ext}}]$, $[\boldsymbol{X}, \boldsymbol{Q_{abs}}]$, $[\boldsymbol{X}, \boldsymbol{Q_{sca}}]$, $[\boldsymbol{X}, \boldsymbol{g}]$ respectively, and then the optical properties were calculated using the well trained SVM model. The comparative results of SVM and MSTM are discussed in Section 4.

4. Comparative results of SVM and MSTM

Firstly, fixing refractive index $m = 1.95 + 0.79i$ [27,38,57] and $a = 0.02um$, the applicability of machine learning was studied. $300nm \le \lambda \le 3100$ nm was investigated. The step size of $\Delta\lambda = 100nm$ was chosen when $\lambda \le 400nm$, while $\Delta\lambda = 150nm$ and $\Delta\lambda = 500nm$ were selected for $550nm \le \lambda < 1600nm$ and $1600nm \le \lambda < 3100nm$ respectively. To parametrize the optical properties with a function of morphological parameters, the monomers number was varied in steps of 10 with $10 \le n_s \le 600$, fractal dimension in steps of 0.1 with $1.8 \le D_f \le 2.2$ and prefactor in steps of 0.1 with $1.2 \le k_0 \le 1.6$.

Figs. 3–4 show the comparative results of MSTM and SVM for different fractal dimensions. As shown in Fig. 4, the results of MSTM may be vary over a small range, this is because there are many particle configurations that satisfy the identical statistical scaling law. However, the SVM can greatly fit the results of MSTM and reflect the general optical properties of BC aggregates.

For evaluating the capacity of SVM to predict the optical properties of BC aggregates whose fractal parameters are not in the training dataset, the comparative results of MSTM and SVM for different wavelengths ($\lambda = 670, 870, 1020nm$) with $D_f = 1.8$, $k_0 = 1.37$ are shown in Fig. 5. The results of MSTM were averaged over 8 realizations to reflect the general optical properties of BC aggregates. As shown in Fig. 5, there are great agreements in integral optical properties between MSTM and SVM. In addition, it verifies the results of SVM can reflect the general optical properties of BC aggregates.

However, as shown in Fig. 6, the SVM method may introduce large errors when the fractal parameters are beyond the scope of training dataset (the results of SVM greatly deviate when $n_s \ge 600$). This is caused by the parametric overfitting, which can be solved by fine tuning of SVM model parameters, However, the tuning is a tricky process. Another good solution is adding a few training data to cover the whole parameter range. To predict the optical properties of BC aggregates in which $620 \le n_s \le 3000$, we added the results of $n_s = 620, 800, 1000, 1500, 2000, 3000$ as training data. Fig. 7 shows the results of SVM are in good agreement with the MSTM after adding a small number of training data.

To evaluate the relative errors, the results of MSTM were averaged over 8 realizations. The relative errors between MSTM and SVM are shown in Fig. 8. The relative errors of Q_{ext}, Q_{abst}, Q_{sca} and ASY are within 2.3%, 1.4%, 5% and 4.8% respectively. The errors are acceptable because the MSTM results may fluctuate from mean values over a small range. In addition, the training data can be decreased by finding better parameters for SVM model to reduce computation time. Therefore, the calculation of optical properties can be simplified by adding a few training data on the basis of pre-trained SVM model. It indicates the SVM is very useful

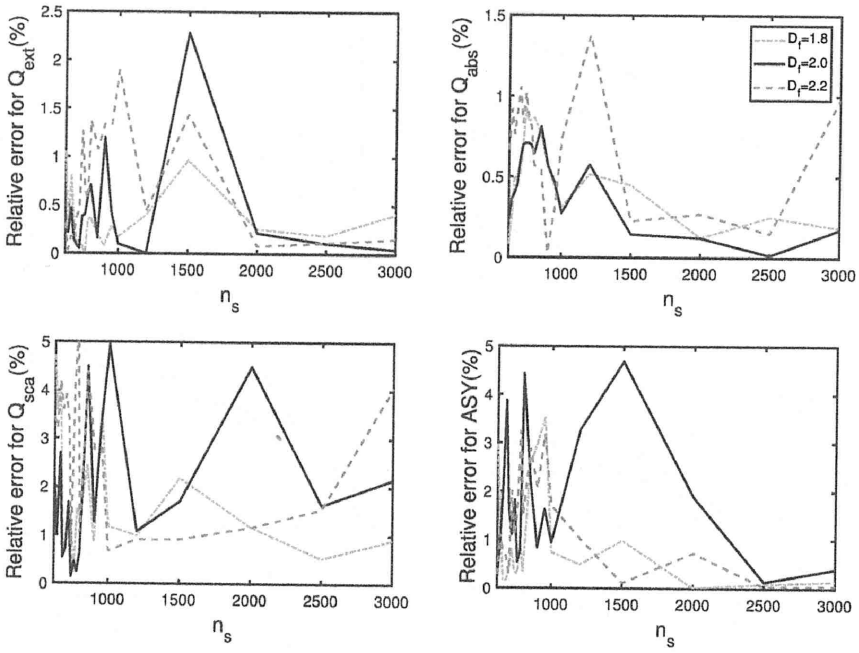

Fig. 8. Relative errors between MSTM and SVM, $\lambda = 1000nm$, $k_0 = 1.2$, $a = 20nm$, $m = 1.95 + 0.79i$.

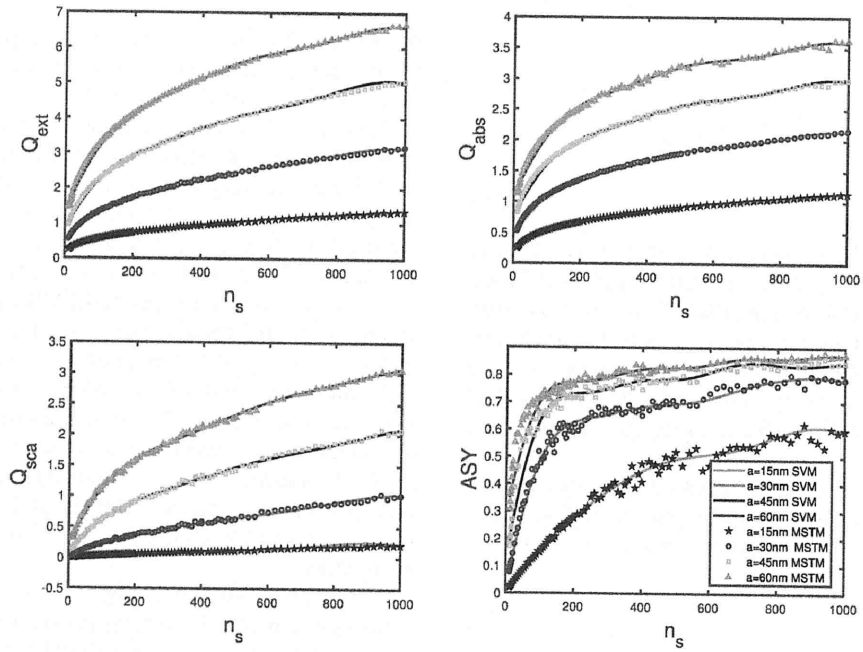

Fig. 9. Comparative results of MSTM and SVM for different monomer radius, $\lambda = 1000nm$, $k_0 = 1.2$, D_f=2.2, $m = 1.95 + 0.79i$.

for calculations of large particles which are not easy handled by MSTM, especially for calculation of lognormal distribution of BC, by setting very small number of training data for large BC.

Furthermore, due to the fact that results of machine learning is only related to training data but not limited to the range of morphology of BC, machine learning may be also applicable to other monomer radius. Fig. 9 is used to verify the applicability of machine learning to different monomer radius. To show the advantages of machine learning for simplifying the calculation, when $n_s > 600$, there is only $n_s = 700, 1000$ in training dataset. As demonstrated in Fig. 9, there are also great agreements between SVM and MSTM for different monomer radius.

The applicability of SVM for other refractive indices are demonstrated in Fig. 10. Following the values given by Bond and Bergstrom [11], we considered other 4 typical refrective indices:$m = 1.75 + 0.63i$, $1.80 + 0.67i$, $1.85 + 0.71i$, $1.90 + 0.75i$. As expected, the results of SVM and MSTM for different refractive indices are also in good agreement. Consequently, machine learning is a versatile approach. In addition, based on the wide applicability of machine learning, it is reasonable to infer that machine learning may be also suitable for more complex morphology, such as BC mixed with other chemical components. Therefore, machine learning is promising for parameterization of optical properties of BC.

5. Discussions and future work

Machine learning was applied in this work for calculation of optical properties of BC aerosols. It gives a new method for parameterizations of optical properties. There are great agreements between SVM and MSTM, as well, SVM can reflect general properties. In addition, applicability of machine learning is only related to training data but not limited by the range of morphological

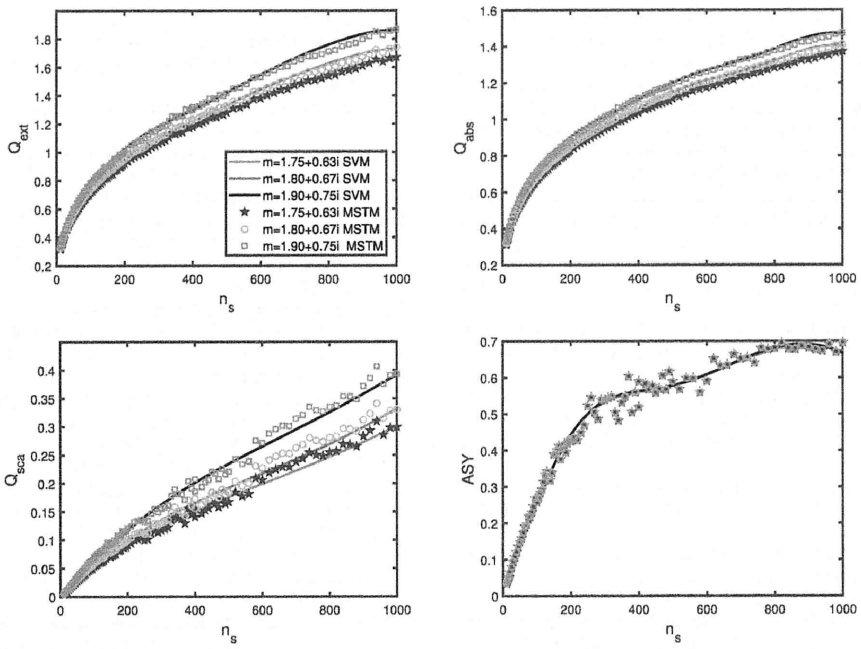

Fig. 10. Comparative results of MSTM and SVM for different refractive indices, $\lambda = 1000nm$, $k_0 = 1.2$, D_f=2.2, $a = 20nm$.

parameters. Therefore, it is also possible to apply this method to more complex morphologies. Although machine learning may provide inaccurate results when the estimated parameters are beyond the range of training data, it can be solved by adding small number of training data. In application, the training dataset can be set as: (1) more training data can be set for BC with the small size parameters, which can be handled easily by the MSTM method; (2) less training data are needed when the size parameters are beyond a threshold value, as is demonstrated in this study. Therefore, it is helpful for improving the computational efficiency. Moreover, the inaccurate results are caused from overfittings of model parameters. It can be also solved by improving the machine learning algorithm. In addition, the trained SVM model can be expressed as linear combination of kernel functions, so it is feasible to apply the method to atmospheric models. Therefore, machine learning is a promising method for the estimation of integral optical properties of BC aerosols.

However, due to the fact that this study is our first try to apply machine learning to calculate optical properties of BC, our study is by no means exhaustive. For example, it would be necessary to investigate the applicability of more complex morphologies, such as BC mixed with other components. In addition, we just apply machine learning to calculate the optical properties of BC aggregates, while how machine learning is coupled in atmospheric models is not involved at present. As for the fact that the SVM may provide inaccurate results when fractal parameters are beyond the corresponding range of training data, we added small number of data to cover the full range. However, it may be still a little inconvenient. Therefore, a machine learning algorithm that can handle morphological parameters beyond corresponding range requires to be studied in the future. Finally, fixed refractive index is assumed in this work. Although this work has verified that machine learning is also applicable for other refractive indices, for application, it is worth noting that the refractive indices are a function of wavelength in reality.

This work may be helpful for climate studies, optical inversions and other fields involved in calculations of lognormal distribution of BC aggregates.

Acknowledgments

We particularly thank Dr. D. W. Mackowski and Dr. M. I. Mishchenko for the MSTM code and the constructive suggestions of reviewers. This work was financially supported by the National Natural Science Foundation of China under grant no. 41675024 and grant no. U1733126, National Key Research and Development Plan under grant no.2016YFC0800100, and Anhui Provincial Key Research and Development Program under grant no. 1704a0902030. We also acknowledge the support of supercomputing center of USTC. The authors gratefully acknowledge all of these supports.

References

[1] Bond TC, Doherty SJ, Fahey DW, Forster PM, Berntsen T, DeAngelo BJ, et al. Bounding the role of black carbon in the climate system: a scientific assessment. J Geophys Res-Atmos 2013;118(11):5380–552. doi:10.1002/jgrd.50171. ⟨Go to ISI⟩://WOS:000325212600025.
[2] Liu DT, Whitehead J, Alfarra MR, Reyes-Villegas E, Spracklen DV, Reddington CL, et al. Black-carbon absorption enhancement in the atmosphere determined by particle mixing state. Nat Geosci 2017;10(3). 184–U132 ⟨Go to ISI⟩://WOS:000395791400009.
[3] Sorensen CM. Light scattering by fractal aggregates: a review. Aerosol Sci Technol 2001;35(2):648–87. ⟨Go to ISI⟩://WOS:000170467100003.
[4] Andreae MO, Jones CD, Cox PM. Strong present-day aerosol cooling implies a hot future. Nature 2005;435(7046):1187–90. doi:10.1038/nature03671. ⟨Go to ISI⟩://WOS:000230140500033.
[5] Anderson TL, Charlson RJ, Schwartz SE, Knutti R, Boucher O, Rodhe H, et al. Climate forcing by aerosols - a hazy picture. Science 2003;300(5622):1103–4. doi:10.1126/science.1084777. ⟨Go to ISI⟩://WOS:000182886500030.
[6] He C, Liou KN, Takano Y, Zhang R, Zamora ML, Yang P, et al. Variation of the radiative properties during black carbon aging: theoretical and experimental intercomparison. Atmos Chem Phys 2015;15(20):11967–80. ⟨Go to ISI⟩://WOS:000364316800029.
[7] Kaufman YJ, Tanre D, Boucher O. A satellite view of aerosols in the climate system. Nature 2002;419(6903):215–23. ⟨Go to ISI⟩://WOS:000177931200051.
[8] Mishchenko MI, Videen G, Babenko VA, Khlebtsov NG, Wriedt T. T-Matrix theory of electromagnetic scattering by particles and its applications: a comprehensive reference database. J Quant Spectrosc Radiat Transfer 2004;88(1–3):357–406. ⟨Go to ISI⟩://WOS:000223415600032.
[9] Luck H. Remarks on the state of the art in automatic fire detection. Fire Saf J 1997;29(2–3):77–85. ⟨Go to ISI⟩://WOS:A1997YC90900002.
[10] Xie QY, Zhang HP, Wan YT, Zhang YM, Qiao LF. Characteristics of light scattering by smoke particles based on spheroid models. J Quant Spectrosc Radiat Transfer 2007;107(1):72–82. ⟨Go to ISI⟩://WOS:000247505900006.

[11] Bond TC, Bergstrom RW. Light absorption by carbonaceous particles: an investigative review. Aerosol Sci Technol 2006;40(1):27–67. doi:10.1080/02786820500421521. ⟨Go to ISI⟩://WOS:000233906000001.
[12] Mishchenko MI, Travis LD, Lacis AA. Scattering, absorption, and emission of light by small particles. Cambridge; New York: Cambridge University Press; 2002. ISBN 052178252X. Tableofcontentshttp://www.loc.gov/catdir/toc/cam031/2002510635.htmlPublisherdescriptionhttp://www.loc.gov/catdir/description/cam0210/2002510635.html.
[13] Xu YL. Calculation of the addition coefficients in electromagnetic multisphere-scattering theory. J Comput Phys 1996;127(2):285–98. ⟨Go to ISI⟩://WOS:A1996VF91200004.
[14] Xu YL, Gustafson BAS. A generalized multiparticle mis-solution: further experimental verification. J Quant Spectrosc Radiat Transfer 2001;70(4–6):395–419. ⟨Go to ISI⟩://WOS:000169975700004.
[15] Mackowski DW, Mishchenko MI. A multiple sphere T-matrix Fortran code for use on parallel computer clusters. J Quant Spectrosc Radiat Transfer 2011;112(13):2182–92. ⟨Go to ISI⟩://WOS:000294518300013.
[16] Mishchenko MI, Liu L, Travis LD, Lacis AA. Scattering and radiative properties of semi-external versus external mixtures of different aerosol types. J Quant Spectrosc Radiat Transfer 2004;88(1–3):139–47. ⟨Go to ISI⟩://WOS:000223415600015.
[17] Draine BT, Flatau PJ. Discrete-dipole approximation for scattering calculations. J Opt Soc Am A-Opt Image Sci Vis 1994;11(4):1491–9. ⟨Go to ISI⟩://WOS:A1994NE24300032.
[18] Laczik Z. Discrete-dipole-approximation-based light-scattering calculations for particles with a real refractive index smaller than unity. Appl Opt 1996;35(19):3736–45. ⟨Go to ISI⟩://WOS:A1996UW46000056.
[19] Mie G. Beitrge zur optik trber medien, speziell kolloidaler metallsungen. Annalen Der Physik 1908;330(3):377–445. doi:10.1002/andp.19083300302.
[20] Liu L, Mishchenko MI, Arnott WP. A study of radiative properties of fractal soot aggregates using the superposition T-matrix method. J Quant Spectrosc Radiat Transfer 2008;109(15):2656–63. ⟨Go to ISI⟩://WOS:000259661500014.
[21] Liu L, Mishchenko MI. Effects of aggregation on scattering and radiative properties of soot aerosols. J Geophys Res-Atmos 2005;110(D11). ⟨Go to ISI⟩://WOS:000229988800009.
[22] Wu Y, Cheng TH, Zheng LJ, Chen H, Xu H. Single scattering properties of semi-embedded soot morphologies with intersecting and non-intersecting surfaces of absorbing spheres and non-absorbing host. J Quant Spectrosc Radiat Transfer 2015;157:1–13. ⟨Go to ISI⟩://WOS:000353083400001.
[23] Kahnert M, Nousiainen T, Lindqvist H. Models for integrated and differential scattering optical properties of encapsulated light absorbing carbon aggregates. Opt Express 2013;21(7):7974–93. ⟨Go to ISI⟩://WOS:000317659300015.
[24] Yon J, Bescond A, Liu F. On the radiative properties of soot aggregates- part 1: necking and overlapping. J Quant Spectrosc Radiat Transfer 2015;162:197–206. ⟨Go to ISI⟩://WOS:000357543800021.
[25] Liu FS, Yon J, Bescond A. On the radiative properties of soot aggregates - part 2: effects of coating. J Quant Spectrosc Radiat Transfer 2016;172:134–45. ⟨Go to ISI⟩://WOS:000373250400012.
[26] Luo J, Zhang YM, Zhang QX. A model study of aggregates composed of spherical soot monomers with an acentric carbon shell. J Quant Spectrosc Radiat Transfer 2018;205:184–95. ⟨Go to ISI⟩://WOS:000417665000021.
[27] Smith AJA, Grainger RG. Simplifying the calculation of light scattering properties for black carbon fractal aggregates. Atmos Chem Phys 2014;14(15):7825–36. ⟨Go to ISI⟩://WOS:000341103600010.
[28] Kahnert M. Modelling the optical and radiative properties of freshly emitted light absorbing carbon within an atmospheric chemical transport model. Atmos Chem Phys 2010;10(3):1403–16. ⟨Go to ISI⟩://WOS:000274410000036.
[29] Kahnert M. Numerically exact computation of the optical properties of light absorbing carbon aggregates for wavelength of 200 nm-12.2 mu m. Atmos Chem Phys 2010;10(17):8319–29. ⟨Go to ISI⟩://WOS:000281845800013.
[30] Pandey A, Chakrabarty RK, Liu L, Mishchenko MI. Empirical relationships between optical properties and equivalent diameters of fractal soot aggregates at 550 nm wavelength. Opt Express 2015;23(24):A1354–62. ⟨Go to ISI⟩://WOS:000366614100002.
[31] Liou KN, Takano Y, He C, Yang P, Leung LR, Gu Y, et al. Stochastic parameterization for light absorption by internally mixed bc/dust in snow grains for application to climate models. J Geophys Res-Atmos 2014;119(12):7616–32. ⟨Go to ISI⟩://WOS:000340247000035.
[32] Cortes C, Vapnik V. Support-vector networks. Mach Learn 1995;20(3):273–97. ⟨Go to ISI⟩://WOS:A1995RX35400003.
[33] Hentschel HGE. Fractal dimension of generalized diffusion-limited aggregates. Phys Rev Lett 1984;52(3):212–15. ⟨Go to ISI⟩://WOS:A1984RY26700013.
[34] Thouy R, Jullien R. A cluster-cluster aggregation model with tunable fractal dimension. J Phys A-Math General 1994;27(9):2953–63. ⟨Go to ISI⟩://WOS:A1994NM53200012.
[35] Wozniak M, Onofri FRA, Barbosa S, Yon J, Mroczka J. Comparison of methods to derive morphological parameters of multi-fractal samples of particle aggregates from TEM images. J Aerosol Sci 2012;47:12–26. ⟨Go to ISI⟩://WOS:000302846500002.
[36] Woniak M. Characterization of nanoparticle aggregates with light scattering techniques. Thesis; 2012.
[37] Jensen MH, Levermann A, Mathiesen J, Procaccia I. Multifractal structure of the harmonic measure of diffusion-limited aggregates. Phys Rev E 2002;65(4). ⟨Go to ISI⟩://WOS:000175146500028.
[38] Wu Y, Cheng TH, Zheng LJ, Chen H. Models for the optical simulations of fractal aggregated soot particles thinly coated with non-absorbing aerosols. J Quant Spectrosc Radiat Transfer 2016;182:1–11. ⟨Go to ISI⟩://WOS:000381321600001.
[39] Wu Y, Cheng TH, Zheng LJ, Chen H. A study of optical properties of soot aggregates composed of poly-disperse monomers using the superposition T-matrix method. Aerosol Sci Technol 2015;49(10):941–9. ⟨Go to ISI⟩://WOS:000366400100005.
[40] Charalampopoulos TT, Shu GC. Effects of polydispersity of chainlike aggregates on light-scattering properties and data inversion. Appl Opt 2002;41(4):723–33. ⟨Go to ISI⟩://WOS:000173500800018.
[41] Yin JY, Liu LH. Influence of complex component and particle polydispersity on radiative properties of soot aggregate in atmosphere. J Quant Spectrosc Radiat Transfer 2010;111(14):2115–26. ⟨Go to ISI⟩://WOS:000280887400009.
[42] Goudeli E, Eggersdorfer ML, Pratsinis SE. Coagulation-agglomeration of fractal-like particles: structure and self-preserving size distribution. Langmuir 2015;31(4):1320–7. doi:10.1021/la504296z. ⟨Go to ISI⟩://WOS:000349059200011.
[43] Kelesidis GA, Goudeli E, Pratsinis SE. Morphology and mobility diameter of carbonaceous aerosols during agglomeration and surface growth. Carbon N Y 2017;121:527–35. ⟨Go to ISI⟩://WOS:000405294400058.
[44] Mackowski DW, Mishchenko MI. Calculation of the T-matrix and the scattering matrix for ensembles of spheres. J Opt Soc Am A-Opt Image Sci Vis 1996;13(11):2266–78. ⟨Go to ISI⟩://WOS:A1996VP77000015.
[45] Mackowski DW. A general superposition solution for electromagnetic scattering by multiple spherical domains of optically active media. J Quant Spectrosc Radiat Transfer 2014;133:264–70. ⟨Go to ISI⟩://WOS:000328868800020.
[46] Liu C, Li J, Yin Y, Zhu B, Feng Q. Optical properties of black carbon aggregates with non-absorptive coating. J Quant Spectrosc Radiat Transfer 2017;187:443–52. ⟨Go to ISI⟩://WOS:000391899300041.
[47] Khalizov AF, Xue HX, Wang L, Zheng J, Zhang RY. Enhanced light absorption and scattering by carbon soot aerosol internally mixed with sulfuric acid. J Phys Chem A 2009;113(6):1066–74. ⟨Go to ISI⟩://WOS:000263134900017.
[48] China S, Scarnato B, Owen RC, Zhang B, Ampadu MT, Kumar S, et al. Morphology and mixing state of aged soot particles at a remote marine free troposphere site: implications for optical properties. Geophys Res Lett 2015;42(4):1243–50. ⟨Go to ISI⟩://WOS:000351851900035.
[49] He CL, Takano Y, Liou KN, Yang P, Li QB, Mackowski DW. Intercomparison of the GOS approach, superposition T-matrix method, and laboratory measurements for black carbon optical properties during aging. J Quant Spectrosc Radiat Transfer 2016;184:287–96. ⟨Go to ISI⟩://WOS:000386982300027.
[50] Keerthi SS, Lin CJ. Asymptotic behaviors of support vector machines with Gaussian kernel. Neural Comput 2003;15(7):1667–89. ⟨Go to ISI⟩://WOS:000183421400011.
[51] Vapnik VN. The nature of statistical learning theory. New York: Springer; 1995. ISBN 0387945598 (New York alk. paper) URL http://magik.gmu.edu/cgi-bin/Pwebrecon.cgi?DB=localFT=22(OCoLC)32703717%22CNT=25+records+per+page.
[52] Crammer K, Singer Y. On the algorithmic implementation of multiclass kernel-based vector machines. J Mach Learn Res 2002;2(2):265–92. doi:10.1162/15324430260185628. ⟨Go to ISI⟩://WOS:000176055300009.
[53] Drucker H, Burges CJ, Kaufman L, Smola AJ, Vapnik V. Support vector regression machines. In: Advances in neural information processing systems; 1997. p. 155–61.
[54] Burges CJC. A tutorial on support vector machines for pattern recognition. Data Min Knowl Discov 1998;2(2):121–67. ⟨Go to ISI⟩://WOS:000076132400002.
[55] Chang CC, Lin CJ. LIBSVM: a library for support vector machines. ACM Trans Intell Syst Technol 2011;2(3). ⟨Go to ISI⟩://WOS:000208617000010.
[56] Richards JS, Hain JD, Vinik HR, Nepomuceno CS, Beckman R. Cross-validation of predictors for a chronic pain control program. Alabama J. Med. Sci. 1982;19(2):120–1. ⟨Go to ISI⟩://WOS:A1982NL76500003.
[57] Bond TC, Bergstrom RW. Light absorption by carbonaceous particles: an investigative review. Aerosol Sci Technol 2006;40(1):27–67. doi:10.1080/02786820500421521. ⟨Go to ISI⟩ ://WOS:000233906000001.